THE JOURNAL OF BIOLOGICAL CHEMISTRY VOL. 280, NO. 47, pp. 39238–39245, November 25, 2005

Glycine Metabolism in Intact Leaves by *in Vivo* ^{13}C and ^{15}N Labeling*

Received for publication, June 28, 2005, and in revised form, August 29, 2005 Published, JBC Papers in Press, September 13, 2005, DOI 10.1074/jbc.M507053200

Lynette Cegelski and Jacob Schaefer[1]

From the Department of Chemistry, Washington University, St. Louis, Missouri 63130

Solid-state ^{13}C NMR measurements of intact soybean leaves labeled by $^{13}CO_2$ (at subambient concentrations) show that excess glycine from the photorespiratory C_2 cycle (*i.e.* glycine not part of the production of glycerate in support of photosynthesis) is either fully decarboxylated or inserted as ^{13}C-labeled glycyl residues in proteins. This ^{13}C incorporation in leaf protein, which is uniformly ^{15}N labeled by $^{15}NH_4{}^{15}NO_3$, occurs as soon as 2 min after the start of $^{13}CO_2$ labeling. In those leaves with lower levels of available nitrogen (as measured by leaf nitrate and glutamine-glutamate concentrations), the excess glycine is used primarily as glycyl residues in protein.

We recently measured photorespiration in soybean leaves by *in vivo* labeling with $^{13}CO_2$ (99 atom % ^{13}C, 200–400 ppm by volume in 21% O_2 and 79% N_2) for 2–8 min, followed by solid-state magic angle spinning ^{13}C NMR detection of the label in the intact, lyophilized leaf (1). A $^{13}C\{^{31}P\}$ rotational-echo double resonance (REDOR)[2] measurement (2) tracked the incorporation of ^{13}C label into intermediates in the Calvin cycle as a function of time. The sensitivity of REDOR to the internuclear separation of a heteronuclear pair of spins (2) was used to determine the fraction of ^{13}C label in the leaf that is within two covalent bonds of ^{31}P, so that the REDOR difference spectrum detected only labeled phosphorylated carbons. This allowed quantification of the ^{13}C isotopic enrichment of the Calvin cycle all of whose participants have a carbon that is two bonds from ^{31}P.

After 2 min of labeling by 300 ppm of $^{13}CO_2$, the protein peaks had the same intensities as those of a leaf at natural abundance in the full-echo spectrum, and the sugar peaks were only slightly enhanced. The 8-rotor cycle $^{13}C\{^{31}P\}$ REDOR difference spectrum, on the other hand, had a significantly enhanced sugar peak intensity, more than five times that of an unlabeled leaf. These spectra indicated that by 2 min after the start of labeling, gas exchange had replaced unlabeled CO_2 within the leaf, and the Calvin cycle intermediates were already at least partially labeled.

By 4 min after the start of labeling, the accumulation of ^{13}C in the full-echo sugar peak was obvious, but the $^{13}C\{^{31}P\}$ REDOR difference peak had not significantly increased. This result indicated that as soon as 2 min after the start of labeling, all $^{12}CO_2$ within the leaf had been replaced by $^{13}CO_2$, and ^{13}C label had been distributed uniformly within ribulose-1,5-bisphosphate (RuBP). However, the ^{13}C isotopic enrichment of RuBP was not 99%, but a lower value that depended on the flux of salvaged photorespiratory unlabeled carbon returned to the Calvin cycle (3) as (phospho)glycerate (Fig. 1). Thus, the isotopic enrichment of the Calvin cycle for a fixed value of the $^{13}CO_2$ concentration determines the ratio of photosynthetic (p) to photorespiratory (r) carbon fluxes, p_c/r_c. The subscripts denote that the ratio of rates is measured by the isotopic enrichment of the Calvin cycle and so all the CO_2 that evolves results from glycerate production. The p_c/r_c ratio was 5.7:1 for both 200- and 300-ppm labeling $^{13}CO_2$ concentrations (1).

The p_c/r_c ratio is the maximum possible value for the ratio of rates of photosynthesis and photorespiration. The ratio is lowered by evolution of additional CO_2 from decarboxylation of glycine (produced in the light) that is not related to production of glycerate and maintenance of the Calvin cycle. The p/r ratio takes all evolved CO_2 into account and was measured by net carbon assimilation rates, which were determined from ^{13}C spin counts converted into total carbon ($^{13}C + {}^{12}C$) by the isotopic enrichments of the Calvin cycle from the REDOR results.

At ambient CO_2 concentration, the p/r ratio was 5.7:1 (1) so that the rate of photorespiratory CO_2 loss was 21% of net CO_2 assimilation, about 80% of the value estimated from Rubisco kinetics parameters (4). At low external CO_2 concentrations, the p/r ratio was less than 5.7:1, but the net carbon assimilation rates indicated that the rate of decarboxylation of glycine was not directly proportional to the oxygenase activity of Rubisco (1) as is commonly assumed (4). That is, the amount of glycerate from the C_2 cycle (Fig. 1) entering the Calvin cycle was not a constant at low CO_2 concentration, but rather decreased, which means that the photorespiratory release of CO_2 resulting from glycerate production (via glycine and serine) also decreased. This, in turn, resulted in the accumulation in the leaf of excess glycine from the oxygenase activity of Rubisco (*i.e.* glycine not used for the production of glycerate).

In this report, we describe the use of solid-state ^{13}C and ^{15}N NMR to correlate carbon and nitrogen metabolism and discover the metabolic fate of excess glycine in the leaf between 2 and 6 min after the start of labeling with $^{13}CO_2$. At subambient CO_2 concentrations, which typically occur as the result of water stress and the associated increased stomatal resistance, we find that a significant fraction of the excess glycine is incorporated into a leaf protein with a high glycine, high α-helix content. We believe that this protein is a structural cell wall component of protoxylem elements used for intercellular water transport (5), and we therefore propose that the photorespiratory C_2 cycle is being used as a CO_2 monitor within the leaf to signal a potential water stress.

MATERIALS AND METHODS

Growth of Soybean Plants—Glycine max (cv. Williams 82) was grown outdoors (June–August 2004) on the roof of the Washington University McMillen Laboratories building. The soybeans were grown in 30-cm diameter pots (6 plants per pot) filled with a mixture of one-third perlite and two-thirds top soil. Approximately 2 weeks after planting, when the first trifoliolates emerged, the pots were fertilized each day with 100 ml

* This work was supported by the National Science Foundation under Grant MCB-0089905. The costs of publication of this article were defrayed in part by the payment of page charges. This article must therefore be hereby marked "*advertisement*" in accordance with 18 U.S.C. Section 1734 solely to indicate this fact.

[1] To whom correspondence should be addressed: Dept. of Chemistry, Washington University, 1 Brookings Dr., St. Louis, MO 63130. Tel.: 314-935-6844; Fax: 314-935-4481; E-mail: jschaefer@wustl.edu.

[2] The abbreviations used are: REDOR, rotational-echo double resonance; CPMAS, cross-polarization magic angle spinning; GDC, glycine decarboxylase; DANTE, acronym for a frequency-selective NMR irradiation scheme using a string of short, weak pulses; RuBP, ribulose-1,5-bisphosphate; Rubisco, ribulose-1,5-bisphosphate carboxylase/oxygenase; ppm, parts per million.

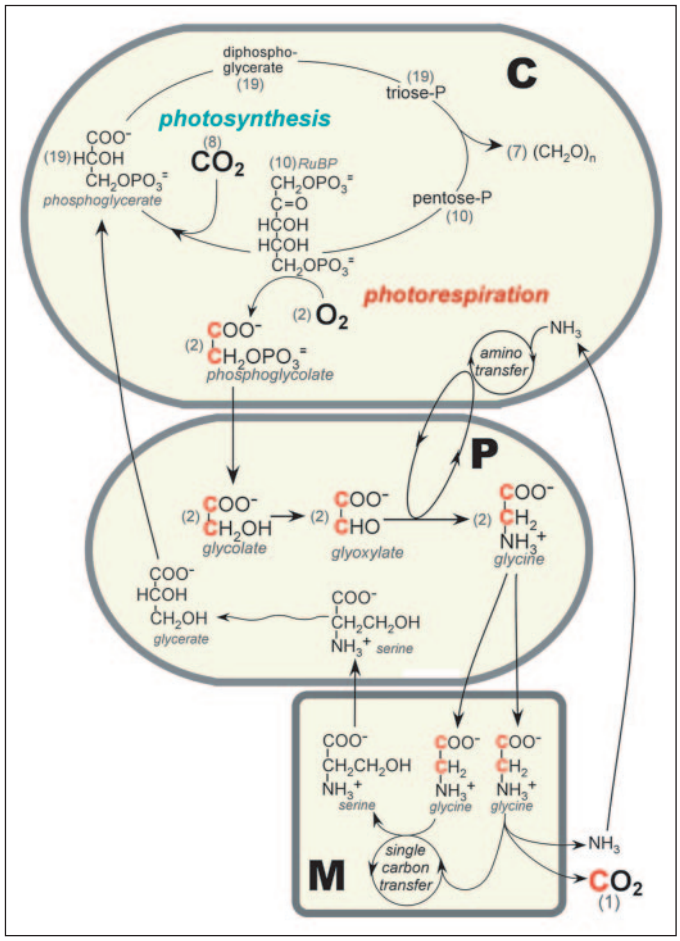

FIGURE 1. **The photorespiratory pathway (adapted from Ogren, Ref. 3).** Oxygenation of RuBP leads to the production of the 2-carbon phosphoglycolate (*red*), which is partially recycled by serine synthesis leading to glycerate. This process requires machinery distributed over three organelles: the chloroplast (*C*), the peroxisome (*P*), and the mitochondrion (*M*). Concurrent energy balance processes via NAD/NADH and ATP/ADP conversions are omitted. The numbers in *parentheses* indicate stoichiometry.

of a 1 g/liter $^{15}NH_4{}^{15}NO_3$ solution. The ^{15}N label (99 atom % ^{15}N, Isotec, Miamisburg, OH) was used to distinguish ^{13}C label in amino acids from that in organic acids and proteins. This high level of fertilizer suppressed symbiotic nitrogen fixation, as evidenced later by the scarcity of root nodules. The ^{15}N enrichment of the leaves was ~50%, as determined by solid-state ^{15}N NMR spin counts (6), less than that of the ammonium nitrate because of unlabeled nitrogen sources in the top soil. The plants were watered by hand, typically every 2 h during the day.

Labeling with $^{13}CO_2$—Labeling with $^{13}CO_2$ (99 atom % ^{13}C) was performed soon after flowers appeared, ~8 weeks after planting. The labeling was performed between 10 AM and 2 PM on August 5, 2004. Details of the labeling have been reported elsewhere (1).

Solid-State NMR—Spectra were obtained using a 6-frequency transmission line probe (7), having a 12-mm long, 6-mm inside diameter analytical coil and a Chemagnetics/Varian magic angle spinning ceramic stator. Lyophilized samples were contained in thin wall Chemagnetics/Varian 5-mm outside diameter zirconia rotors. The rotors were spun at 7143 Hz with the speed under active control to within ±2 Hz. The spectrometer was controlled by a Tecmag pulse programmer. Radiofrequency pulses for ^{31}P (202 MHz), ^{13}C (125 MHz), and ^{15}N (50.3 MHz) were produced by 1-kilowatt American Microwave Technology power amplifiers. Proton (500 MHz) radiofrequency pulses were generated by a 1-kilowatt Amplifier Systems tube amplifiers driven by a 50-watt American Microwave Technology power amplifier. The π-pulse lengths were 6 μs for ^{31}P, 8 μs for ^{13}C, and 9 μs for ^{15}N. A 12-T static magnetic field was provided by an 89-mm bore Magnex superconducting solenoid. Proton-carbon cross-polarization magic angle spinning (CPMAS) transfers were made with radiofrequency fields of 62.5 kHz. Proton dipolar decoupling was 100 kHz during data acquisition.

CPMAS intensities were compared leaf-to-leaf on an absolute basis by normalization with respect to the natural abundance aliphatic carbon signal intensities between 0 and 30 ppm. The normalization reduced the effect of variations between leaves in protein content.

REDOR was used to restore the dipolar couplings between heteronuclear pairs of spins that are removed by magic angle spinning (2). REDOR experiments are always done in two parts, once with rotor-synchronized dephasing pulses (S) and once without (full-echo, S_0). The dephasing pulses change the sign of the heteronuclear dipolar coupling, and this interferes with the spatial averaging resulting from the motion of the rotor. The difference in signal intensity (REDOR difference, $\Delta S = S_0 - S$) for the observed spin in the two parts of the REDOR experiment is directly related to the corresponding distance to the dephasing spin (2). All $^{15}N\{^{31}P\}$ and $^{13}C\{^{15}N\}$ REDOR spectra were collected with standard xy-8 phase cycling (9), on both observed and dephasing channels.

Frequency selective ^{13}C π pulses were generated using the so-called DANTE sequence (10). The ^{13}C radiofrequency was shifted on resonance for the peak to be inverted and 64 rotor-asynchronous 0.5-μs pulses produced an 80% inversion. Following a z-axis $\pi/2$ restoration pulse, a delay of 10 ms was sufficient to equilibrate the populations of directly bonded ^{13}C-^{13}C pairs (11), one member of which had been inverted by the DANTE π pulse. This procedure was used to establish connectivities between ^{13}C labels in early metabolites of photosynthesis and photorespiration.

RESULTS

Glycyl Residues in Protein—The total ^{13}C assimilation in a leaf labeled by 300 ppm of $^{13}CO_2$ for 6 min is determined by subtracting the cross-polarization magic angle spinning ^{13}C NMR spectrum of an unlabeled leaf from that of the labeled leaf (Fig. 2). The dominant peaks in the difference spectrum arise from the -CH_2O- products of the Calvin cycle (65–105 ppm). The major sugar peak occurs at 72.6 ppm (relative to external tetramethylsilane). Non-sugar peaks appear in the carbonyl and methylene carbon regions (in blue) and arise from products of the oxygenase activity of Rubisco.

Two carbonyl carbon peaks are observed in the difference spectrum of Fig. 2. The low field peak centered at 179 ppm (with about a 3-ppm width) is assigned to glycerate, serine, some glycine, and possibly lesser amounts of glycolate (1). None of these carbonyl carbons has a directly bonded nitrogen. The high field carbonyl carbon shift of 171 ppm is characteristic of a glycine carbonyl carbon in a peptide bond in an α-helical local conformation (12). It is not consistent with a carbonyl carbon in a free amino acid or organic acid. The diminution of intensity of the 171-ppm peak following a 1-ms $^{13}C\{^{15}N\}$ REDOR evolution period (inset in red) proves that the carbonyl carbon is directly bonded to nitrogen, and so this peak is assigned to glycyl residues in proteins. The ~35% reduction in intensity is consistent with the 50% ^{15}N isotopic enrichment of all nitrogen in the leaf, and a product of evolution time and dipolar coupling of just over 1 (2).

The methylene carbon peak at 43 ppm also shows $^{13}C\{^{15}N\}$ dephasing (Fig. 2, *red*) and has the α-carbon shift of a glycyl residue (12). In addi-

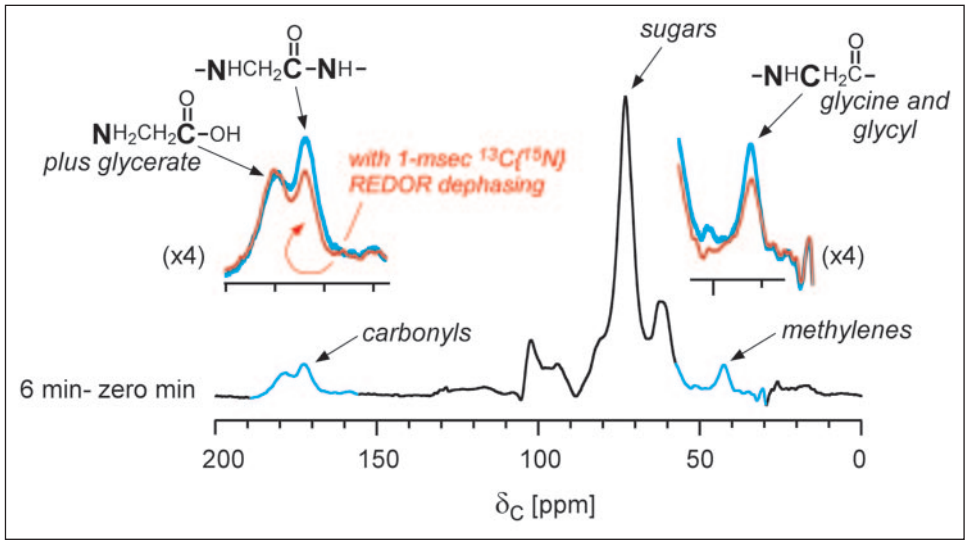

FIGURE 2. **Cross-polarization magic angle spinning ^{13}C NMR spectrum of an intact lyophilized soybean leaf labeled for 6 min with $^{13}CO_2$ at 300 ppm (by volume).** This is a difference spectrum resulting from the subtraction of the spectrum of an unlabeled leaf. Each of the spectra in the difference resulted from the accumulation of 110,000 scans (using a 2-ms matched cross-polarization transfer at 62.5 kHz with a 1.5-s repeat time). The relative scaling of the two spectra was chosen to minimize the natural-abundance difference peaks between 10 and 30 ppm. Only peaks arising from the ^{13}C label remain, and their integration gives an accounting of total ^{13}C assimilation in the leaf during the labeling period. Two carbonyl carbon difference peaks (in *blue*) are observed: one at 179 ppm (near the chemical shift of the carboxyl carbon of free glycine) and the other at 171 ppm (the characteristic chemical shift of the peptide carbonyl carbon of glycyl residues in α-helical local conformations). The 171-ppm peak and a 43-ppm methylene carbon peak (both in *red*) decrease in intensity following a ^{13}C{^{15}N} dipolar evolution period for 1 ms (*insets*), indicating directly bonded ^{13}C-^{15}N pairs.

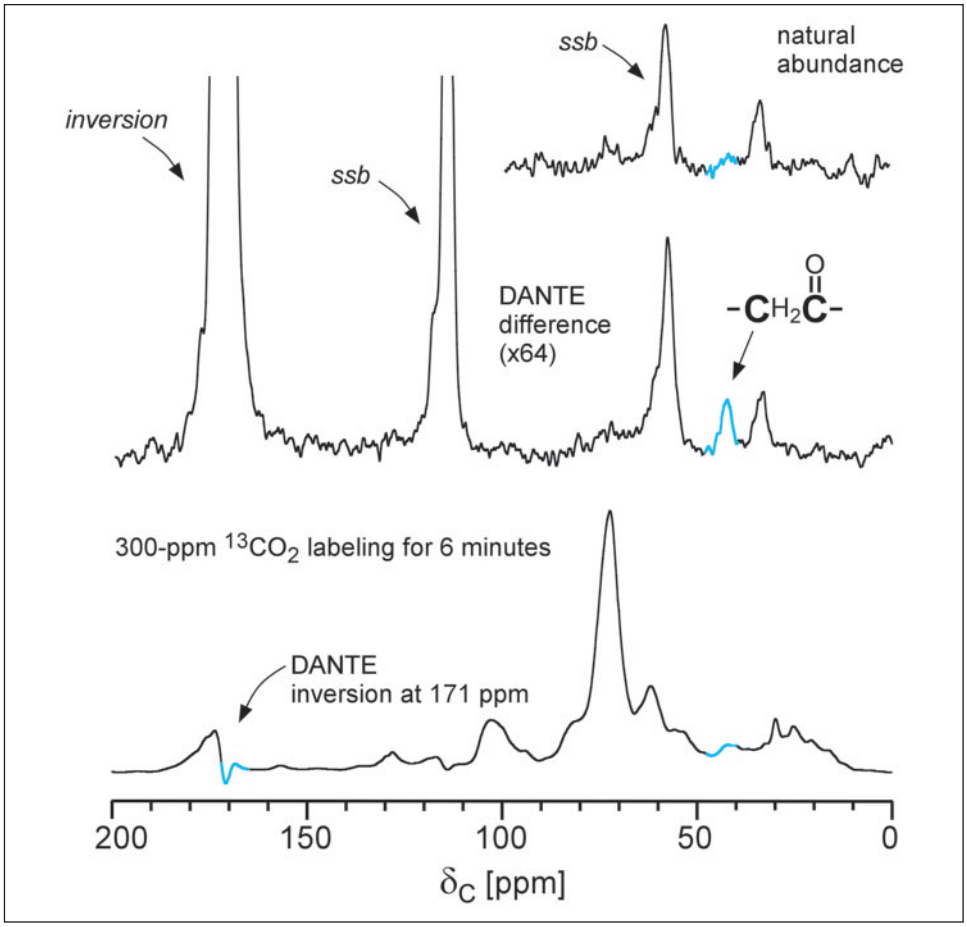

FIGURE 3. *Bottom*, cross-polarization magic angle spinning ^{13}C NMR spectrum of an intact lyophilized soybean leaf labeled for 6 min with $^{13}CO_2$ at 300 ppm (by volume). The carbonyl carbon peak has a maximum at 176 ppm and the shoulder at 171 ppm (most of which is due to natural abundance ^{13}C) has been inverted by a frequency-selective pulse. The difference spectrum at the *top* results from subtracting the bottom spectrum from the corresponding spectrum with no frequency-selected inversion, both obtained after a 10-ms delay for equilibration of spin populations (stored along the static magnetic field) by ^{13}C-^{13}C spin diffusion. Each of the spectra in the difference resulted from the accumulation of 230,000 scans. The difference spectrum shows the inverted shoulder (and its spinning sidebands), together with a peak at 43 ppm arising from ^{13}C directly bonded to the carbonyl carbon ^{13}C with a shift of 171 ppm. The peak at 43 ppm does not appear in the corresponding difference spectrum of an unlabeled leaf (*inset*). Both difference spectra have a peak near 25 ppm, which is assigned to various aliphatic carbons in protein side chains proximate to ester or acid carbonyl carbons in pectins, all at natural abundance. Magic angle spinning was at 7143 Hz.

tion, the 43-ppm methylene carbon peak has a direct link to the 171-ppm carbonyl carbon peak, as established by the results of a selective inversion experiment (Fig. 3). In this experiment, the total ^{13}C signal at 171 ppm (label and natural abundance) is inverted and then stored along the magnetic field by a $\pi/2$ restoration pulse. The inverted population then partially equilibrates with the normal Boltzmann population of ^{13}Cs. The equilibration occurs via dipolar coupling and is complete in 10 ms for a 2-kHz ^{13}C-^{13}C coupling (11). Thus, a positive-going peak in the difference spectrum (Fig. 3, *top*), which does not appear in the corresponding natural abundance difference spectrum (Fig. 3, *inset*), indicates the presence of a ^{13}C-^{13}C double-labeled covalent bond, characteristic of the uniformly labeled products of the Calvin cycle.

The observed ^{13}C-^{15}N and ^{13}C-^{13}C dipolar couplings of Figs. 2 and 3, together with characteristic ^{13}C chemical shifts at 171 and 43 ppm, are only consistent with high concentrations of glycyl residues in leaf protein. Other plausible metabolites have NMR parameters that are not

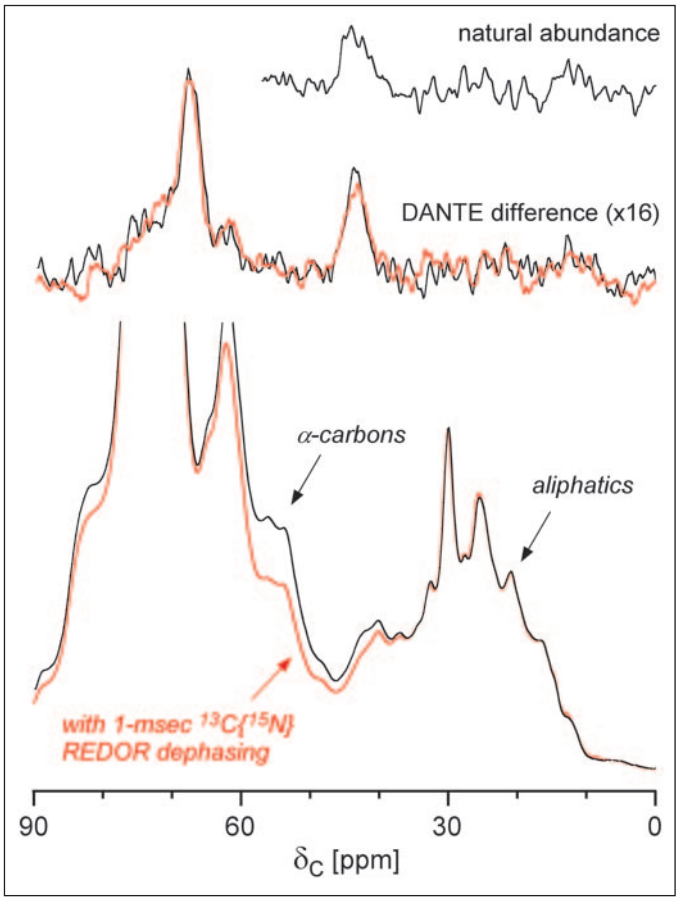

FIGURE 4. *Bottom*, cross-polarization magic angle spinning ^{13}C NMR spectrum of an intact lyophilized soybean leaf labeled for 6 min with $^{13}CO_2$ at 300 ppm (by volume). Only the region of the spectrum between 0 and 90 ppm is shown. The carbonyl carbon shoulder at 181 ppm has been inverted by a frequency selective pulse. The difference spectrum at the *top* results from subtracting the bottom spectrum from the corresponding spectrum with no frequency selected inversion, both obtained after a 10-ms delay for equilibration of spin populations stored along the static magnetic field by ^{13}C-^{13}C spin diffusion. Each of the spectra in the difference resulted from the accumulation of 230,000 scans. The difference spectrum shows a methylene carbon peak at 43 ppm that is larger than that observed in the corresponding difference spectrum of an unlabeled leaf (*inset*). The superimposed spectra in *red* were taken with a 1-ms $^{13}C\{^{15}N\}$ dipolar evolution period following the 10-ms period for ^{13}C-^{13}C spin diffusion and preceding acquisition. Diminution of signal intensity indicates the presence of directly bonded ^{13}C-^{15}N pairs.

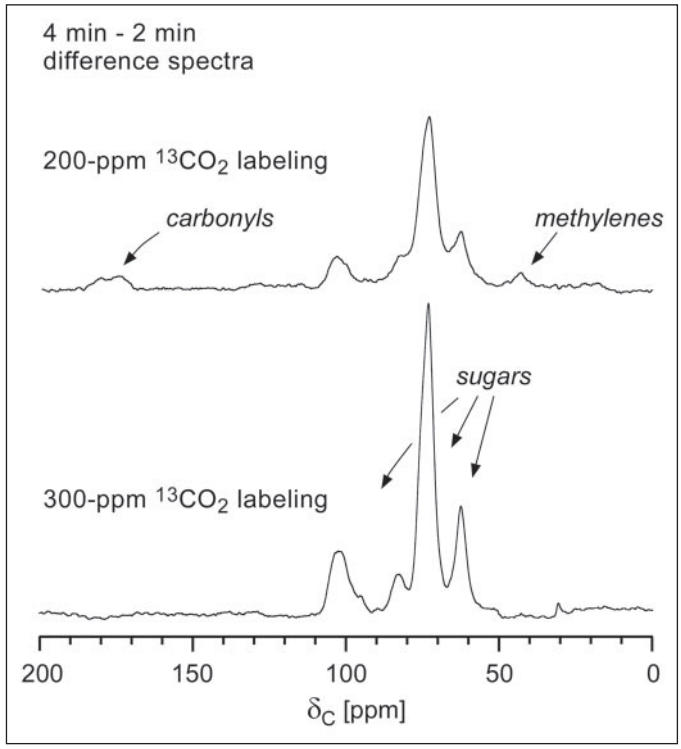

FIGURE 5. **Cross-polarization magic angle spinning ^{13}C NMR spectrum of intact lyophilized soybean leaves labeled for 4 min with $^{13}CO_2$ at 200 ppm (*top*) and 300 ppm (*bottom*).** Both are difference spectra resulting from the subtraction of the corresponding spectra of leaves labeled for 2 min. Each of the spectra of the two differences resulted from the accumulation of 20,000 scans. The difference spectrum of the leaf labeled with 300 ppm of $^{13}CO_2$ shows no accumulation of ^{13}C label in carbonyl carbons between 2 and 4 min of the start of the labeling period.

observed. Organic acids from the tricarboxylic acid cycle, for example, can match the 43-ppm shift of the methylene carbon, but not the 171-ppm shift of the carbonyl carbon or the observed ^{13}C-^{15}N dipolar coupling.

A ^{13}C-^{13}C link of the 43-ppm methylene carbon peak to the 179-ppm carbonyl carbon peak of Fig. 2 is much weaker (Fig. 4, *middle* and *top*) than to the 171-ppm peak (Fig. 3, *middle* and *top*), indicating that more of the 179-ppm peak arises from glycerate (which has no methylene carbon) than from glycine, 6 min after the start of the labeling.

Early Carbon Assimilation—The total carbon assimilation for soybean leaves labeled for just 2 min shows pronounced differences in the routing of label as a function of $^{13}CO_2$ concentration (see Fig. 6 of Ref. 1). At near ambient CO_2 concentration (400 ppm), the dominant carbonyl carbon peak has a 179-ppm shift and is matched in intensity by a 43-ppm peak, both consistent with the presence of free glycine. Previous $^{13}C\{^{31}P\}$ REDOR measurements have shown that a significant amount of labeled glycerate has not accumulated by 2 min after the start of labeling (1). At subambient $^{13}CO_2$ concentrations, the glycine peak decreases in intensity and the 171-ppm glycyl peptide peak increases. As the carboxylase activity of the Calvin cycle decreases, the demand for glycerate decreases and the apparent immediate metabolic response is a rerouting of free glycine away from glycerate production and into protein synthesis.

This rerouting is also seen for the leaf labeled by 200 ppm of $^{13}CO_2$ for 4 min. The difference spectrum for that leaf, obtained by subtracting the spectrum of the leaf labeled for 2 min, has a pronounced 171-ppm peptide carbonyl carbon peak (Fig. 5, *top*). The leaf labeled by 300 ppm of $^{13}CO_2$ for 4 min, on the other hand, is significantly different: no carbonyl carbon peak at all appears in the difference spectrum (Fig. 5, *bottom*). We will discuss this comparison in more detail after we present the nitrogen assimilation results in the next two subsections.

Nitrogen Assimilation—The ^{15}N NMR spectra of two $^{13}CO_2$-labeled soybean leaves are shown in Fig. 6. These are REDOR full-echo spectra after a 29-ms evolution period so the intensities of protonated nitrogens are reduced somewhat relative to those of non-protonated nitrogens (13). Nevertheless, familiar assignments of peaks (13, 14) to protein main chain and lysine, arginine, and histidine side chain nitrogens, and to ribosomal RNA purines, are easily made (*arrows*, Fig. 6, *middle*).

There are virtually no variations in the relative intensities of peaks arising from these structural nitrogens from one leaf to another. There are, however, significant variations in the intensities of the peaks associated with the dynamic metabolic nitrogen pools of nitrate and glutamine-glutamate. The nitrate peak appears at 350 ppm (15) and the glutamine-glutamate amine peak at 30 ppm (15–17). The amine nitrogen has the same shift in both glutamine and glutamate. The glutamine amide-nitrogen shift is obscured by the massive 95-ppm peptide nitrogen peak. The top and middle spectra of Fig. 6 illustrate the extremes observed in the leaf-to-leaf metabolic nitrogen pools for plants grown in

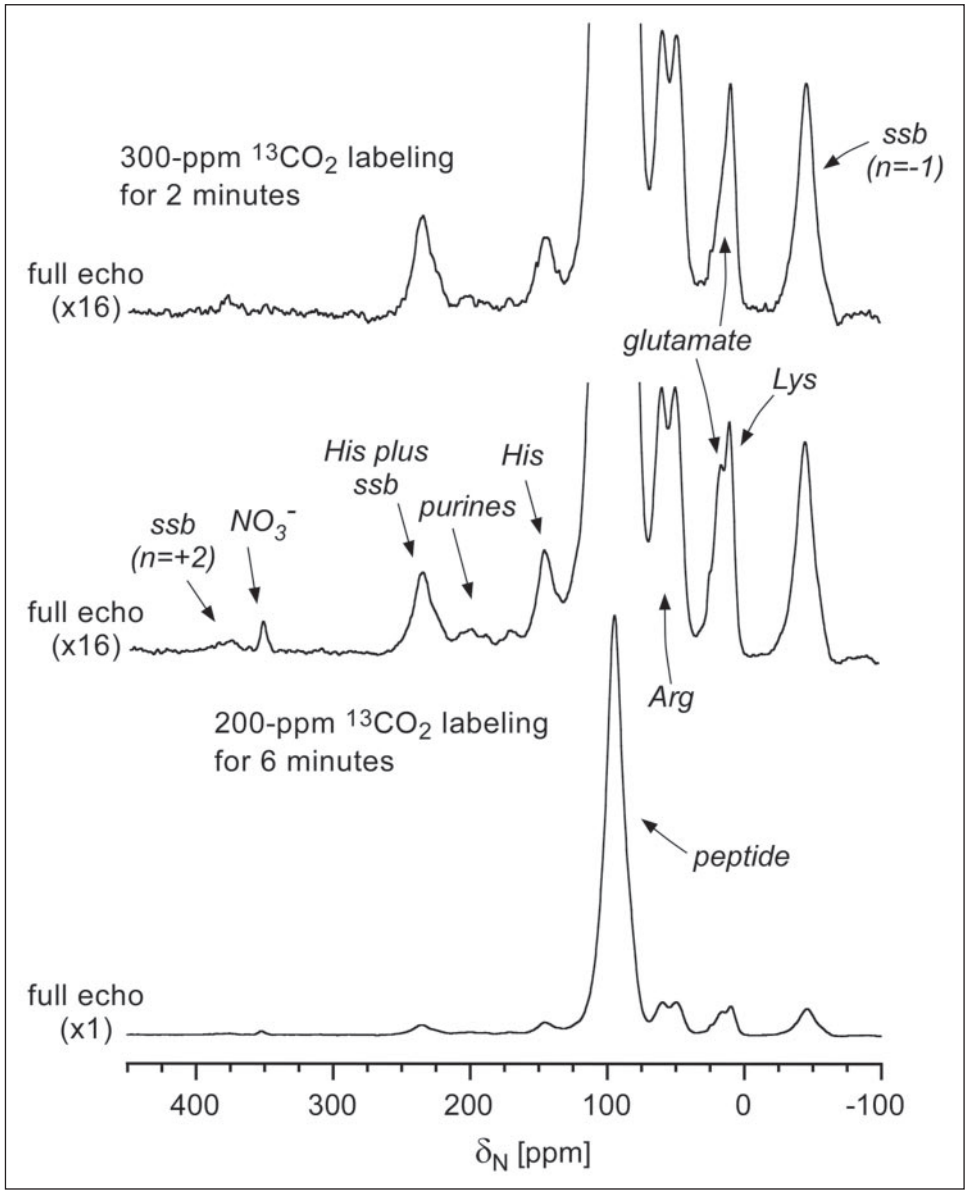

FIGURE 6. **$^{15}N\{^{31}P\}$ 208 rotor-cycle REDOR full-echo spectra of lyophilized soybean leaves labeled with 200 ppm of $^{13}CO_2$ for 6 min (*bottom*) and with 300 ppm of $^{13}CO_2$ for 6 min (*top*).** The spectra have been scaled for equal intensities of the peptide nitrogen peak. The intensities of the peaks identified by *arrows* in the expansion of the bottom spectrum (shown in the *middle* of the figure) varied little from one leaf to another, with two exceptions: the nitrate peak (350 ppm) and the glutamine-glutamate amino nitrogen peak (30 ppm). The chemical shifts are relative to external solid ammonium sulfate as a reference. The ammonium sulfate resonance is at +20 ppm relative to liquid ammonia as a reference. Each of the full-echo spectra resulted from the accumulation of 50,000 scans (using a 2-ms matched cross-polarization transfer at 50 kHz with a 1.5-s repeat time). Magic angle spinning was at 7143 Hz.

TABLE ONE

^{15}N incorporation in leaves labeled by $^{13}CO_2$ for short times

Labeling conditions, $^{13}CO_2$	95-ppm peptide $^{15}N\{^{31}P\}\Delta S/S_0$[a]	Nitrate relative to peptide amide[b]	Glutamine-glutamate amine relative to peptide amide[c]	Relative total ^{15}N incorporation
ppm/min				
400/2[d]	0.014	1.0	0.76	0.69
300/2[d]	0.017	0.5	0.44	0.70
200/4[d]	0.019	1.4	0.62	1.00
200/2[e]	0.021	1.6	0.75	1.08
200/2[d]	0.022	1.5	0.62	1.00
1000/4[f]	0.023	1.0	0.56	1.39
300/4[d]	0.024	1.0	0.94	0.60
400/2[e]	0.025	2.2	0.90	1.20
Natural abundance[e]	0.026	3.0	1.00	1.21
1000/2[f]	0.028	0.6	0.54	1.49

[a] 29-ms dipolar evolution from 208 rotor cycles with magic angle spinning at 7143 Hz.
[b] Nitrate signal intensity relative to peptide second ($n = +2$) spinning-sideband intensity.
[c] Glutamine-glutamate amine intensity relative to peptide first ($n = -1$) spinning-sideband intensity.
[d] From 2004 $^{13}CO_2$ labeling experiments (Ref. 1).
[e] From 2001 $^{13}CO_2$ labeling experiments on plants ^{15}N-labeled similarly to those in 2004.
[f] From 2003 exposure to $^{12}CO_2$ for plants ^{15}N-labeled similarly to those in 2004.

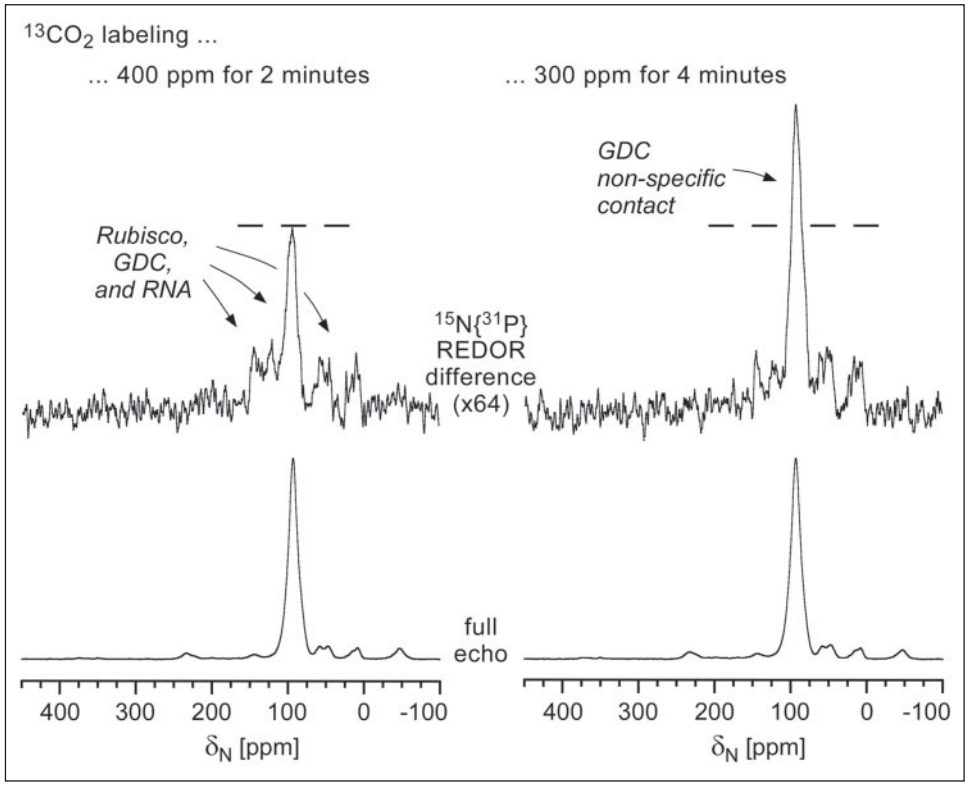

FIGURE 7. **$^{15}N\{^{31}P\}$ 208 rotor-cycle REDOR spectra of lyophilized soybean leaves labeled with 400 ppm $^{13}CO_2$ for 2 min (*left*) and 300 ppm $^{13}CO_2$ for 4 min (*right*).** The full-echo spectra are shown at the *bottom* of the figure and the REDOR difference spectra (full-echo minus dephased echo) at the *top*. The full-echo and dephased-echo spectra of the REDOR experiment on the *left* each resulted from the accumulation of 50,000 scans, and those of the experiment on the right, 75,000 scans. Magic angle spinning was at 7143 Hz.

2004. Qualitative levels of metabolic nitrogen pools are summarized in TABLE ONE, along with the total ^{15}N content, for leaves exposed to a variety of $^{13}CO_2$ labeling concentrations on plants grown in three different summers.

$^{15}N\{^{31}P\}$ REDOR—The $^{15}N\{^{31}P\}$ REDOR dephasing ($\Delta S/S_0$) for a dipolar evolution time of about 30 ms arises from all ^{15}N that is within 10 Å of ^{31}P (13). For phosphorylated lysines and arginines, both side chain and main chain nitrogens contribute to the REDOR difference. A single ^{31}P within the binding site of a uniformly ^{15}N-labeled 50-kDa protein will result in contributions to a REDOR difference signal from 5–10 main chain nitrogens so that the 95-ppm $\Delta S/S_0 \approx .01$ (14). Rubisco and glycine decarboxylase (GDC) are by far the most abundant proteins in the leaf (18) and so the $^{15}N\{^{31}P\}$ REDOR dephasing for the most part reports on the extent of contact of these proteins with phosphorous. Leaf-to-leaf variation in dephasing is more pronounced for the (primarily) main chain peptide nitrogen peak at 95 ppm than for any of the side chain nitrogens (Fig. 7). Values of the 95-ppm $^{15}N\{^{31}P\}$ dephasing after 29 ms of dipolar evolution for leaves labeled under a variety of CO_2 concentrations are presented in TABLE ONE.

DISCUSSION

Variations in Glycyl Incorporation in Leaf Protein—Two of the leaves of TABLE ONE have a 95-ppm $^{15}N\{^{31}P\}$ $\Delta S/S_0$ that is relatively small, with a value between 0.014 and 0.017. For the leaf labeled by 400 ppm of $^{13}CO_2$ for 2 min ($\Delta S/S_0 = .014$), almost all the ^{13}C label passing through the oxygenase path of Rubisco had been routed to glycine (see Fig. 6 in Ref. 1). There was no significant incorporation of glycyl residues into protein. The leaf was photosynthetically active, considering the extent of label incorporated into sugar in just 2 min. Based on these results, we take an observed 95-ppm $^{15}N\{^{31}P\}$ $\Delta S/S_0$ of about 0.015 as representative of the protein main chain-phosphorous contact for a lyophilized leaf that had fully activated Rubisco and sufficiently activated GDC to convert all of the oxygenase product of Rubisco into glycerate via glycine and the C_2 pathway.

The other low value of $^{15}N\{^{31}P\}$ dephasing ($\Delta S/S_0 = 0.017$) is observed for the leaf labeled by 300 ppm of $^{13}CO_2$ for 2 min. This leaf appeared to be normal, with size and color comparable to those of the other leaves labeled in 2004. Nevertheless, the leaf had unusually small nitrate and glutamine-glutamate metabolic nitrogen pools, as well as a low total incorporation of ^{15}N (TABLE ONE). Perhaps this leaf had been damaged or inadvertently covered or shaded and was somehow developmentally atypical. In any event, the leaf was apparently unable to use the single carbons that result from the total decarboxylation of glycine, for example to synthesize other amino acids (19), and instead incorporated all excess glycine directly into protein (see Fig. 6 of Ref. 1).

The more typical value of the 95-ppm peptide nitrogen $\Delta S/S_0$ for leaves labeled under non-ambient CO_2 concentrations is between 0.019 and 0.028 (TABLE ONE). For example, the REDOR dephasing for the leaf labeled with 300 ppm of $^{13}CO_2$ for 4 min (Fig. 7, *right*) is 0.024, a value which is in the middle of the 0.019 – 0.028 range. This leaf has no observable carbonyl carbon label (Fig. 5, *bottom*), which means that all the product of the oxygenase activity of Rubisco had been decarboxylated. That is, for every two oxygenations of Rubisco in the light, two CO_2 molecules are released, contrary to the conventional assumption in this situation of the release of one CO_2 (4).

Activation of additional GDC for total glycine decarboxylation requires additional ATP (18), which moves sequestered inorganic phosphate into dispersed biophosphate. We attribute the increase in $^{15}N\{^{31}P\}$ peptide dephasing from 0.015 to about 0.025 to adventitious proximity of ATP and GDC in the lyophilized leaf. There is no corresponding increase for the lysine, arginine, and histidine side chain $^{15}N\{^{31}P\}$ dephasing, because there is no increase in the level of phosphorylation of these side chains, and therefore no increase in specific ^{15}N-^{31}P proximities.

Most of the leaves in TABLE ONE appear to have been in a metabolic state characterized by high values of $^{15}N\{^{31}P\}$ $\Delta S/S_0$, including the natural abundance leaf harvested under steady-state conditions in the light.

We conclude therefore that in their normal state, soybean leaves are fully capable of diverting excess glycine from the C_2 pathway into either direct protein synthesis or full decarboxylation.

Leaf Metabolism in Low CO_2—Under normal conditions, the CO_2 concentration within a soybean leaf drops to that of the leaves in TABLE ONE labeled with subambient CO_2 concentrations only as the result of a water stress and the associated increased stomatal resistance and decreased gas diffusivity (20). This combination depletes the CO_2 within the leaf but has little effect on the much more abundant O_2 so that the carboxylase activity of Rubisco is reduced but not the oxygenase activity. The metabolism within the leaf immediately responds to the resulting higher level of glycine (relative to glycerate) by incorporating glycyl residues into protein (Fig. 2), by fully decarboxylating glycine (Fig. 5, *bottom*), or by some combination of the two (Fig. 5, *top*). The specific short term response appears to depend on the status of the nitrogen metabolic pools within the leaf (TABLE ONE) and the extent of GDC activation, presumably in such a way that the net productivity or efficiency of the leaf (or plant) is optimized.

A component of this strategy might include synthesizing protein as part of a protective, fast response by the leaf to an anticipated water stress, well before any internal structural damage has occurred. The basis for this suggestion is that the glycyl residues of Fig. 2 have a carbonyl carbon isotropic chemical shift of 171 ppm. The average shift for glycyl residues in proteins is 174 ppm (21) so that the incorporation of glycine into a variety of local conformations is unlikely. The 171-ppm glycine shift indicates unambiguously an α-helical conformation both in solution and in the solid state (12, 22). A β-sheet conformation might have been expected for a high glycine content protein (23), but the 168-ppm shift for β-sheets is not observed. High concentrations of glycyl residues in α-helical conformations are consistent with the formation of glycine-rich protein (GRP), a cell wall structural protein often found localized in xylem elements used for intercellular water transport (5). GRPs can have glycine contents representing up to 60–70% of all amino acid residues (23), and in some instances have been identified with secondary structures matching that of α-helical collagen (5). Additional experiments are needed to confirm these preliminary assignments and conclusions.

Plant Growth in High CO_2—Atmospheric CO_2 levels are anticipated to be 550 ppm (by volume) in about 40 years (24), which should lead to increased photosynthetic activity. Increased levels of nitrogen within the plant, achieved either by fertilization or by increased rooting volumes for N_2-fixing plant systems, should then lead to enhanced plant productivity by matching increased carbon assimilation with increased nitrogen assimilation (25, 26). However, in experiments with high CO_2 concentrations, the expected theoretical gain in productivity has not been realized, at least not for soybeans grown in the open field (no artificial canopies, no root constraints, no nitrogen limitations) under 550 ppm of free-air CO_2-enhanced conditions (27). The deficit in productivity appears to be correlated with insufficient levels of the RuBP substrate for Rubisco (27).

One possible explanation for the deficit is that the observed long term dependence of nitrate assimilation on photorespiration, possibly via the production of NADH in the peroxisome, is a limiting factor (28). A reduction in photorespiration means a reduction in nitrate assimilation, which could lead to reduced carbon utilization including protein synthesis. With this explanation, however, the connection to limiting RuBP is not immediately obvious.

We offer another possibility based on our observation (from ^{13}C isotopic enrichment measurements) at ambient and subambient CO_2 concentrations that the rate of turnover of the Calvin cycle is directly proportional to the demand for glycerate returned from the C_2 cycle: slower turnover, less glycerate; faster turnover, more glycerate (1). If all of the glycine produced by Rubisco oxygenation indeed fueled glycerate production and Calvin cycle turnover, then other pathways for C_2 glycine use, including full decarboxylation (see Fig. 5), would be limited. Reduced respiratory decarboxylation could ultimately result in reduced nitrate assimilation (19). There is no sign of such a single purpose use of glycine in the high CO_2 $^{15}N\{^{31}P\}$ REDOR dephasing results of TABLE ONE. The observed $\Delta S/S_0$ values of 0.023 and 0.028 suggest fully active GDC. At 550 ppm of CO_2 therefore, the combination of increased Rubisco carboxylase activity and decreased oxygenase activity (25) means that there is not enough glycerate returning from the C_2 pathway to maintain fully the increased turnover rate of the Calvin cycle. The limiting factor is therefore the available triose in the Calvin cycle, which is manifest as a shortage of the sugar substrate for Rubisco, RuBP.

Solid-State NMR and Correlation of Carbon and Nitrogen Metabolism in Intact Leaves—Solid-state NMR of an intact, chemically stable, lyophilized leaf allows the detection of all ^{13}C and ^{15}N incorporated in the leaf, regardless of whether the label is in a component that is soluble or insoluble, extractable, or intractable. Besides this accurate spin counting for compositional analysis (17), solid-state measurements of inter-residue ^{13}C-^{15}N dipolar couplings in leaf proteins are important for assignments like the identification of glycyl residues (Fig. 2). These couplings would be lost if the leaf were subjected to conventional extraction and digestion. In addition, observations of *in situ* protein chemical shifts can reveal local conformations (12), and this structural information is also lost if the protein is extracted, even if it is not digested. Finally, although some of the correlations of carbon and nitrogen metabolism obtained from solid-state NMR and discussed above are speculative at this point, the physical proximities and intermolecular dipolar couplings of ^{13}C, ^{15}N, and ^{31}P in metabolites in the leaf are parameters that should help provide the tests of more insightful future correlations. To implement these tests, the leaf must stay intact. Once the tests have been completed, degradative analysis is always an option.

Acknowledgments—We thank Astrid Sivertsen and Robert O'Connor for preliminary 30 MHz ^{15}N NMR measurements on leaves in 2002 and 2003.

REFERENCES

1. Cegelski, L. & Schaefer, J. (2006) *J. Magn. Reson., in press*
2. Gullion, T. & Schaefer, J. (1989) *Adv. Magn. Reson.* **13,** 58–83
3. Ogren, W. L. (1984) *Annu. Rev. Plant Physiol.* **35,** 415–442
4. Sharkey, T. D. (1988) *Physiol. Plant* **73,** 147–152
5. Ringli, C., Keller, B. & Ruser, U. (2001) *Cell Mol. Life Sci.* **58,** 1430–1441
6. Schaefer, J., Stejskal, E. O. & McKay, R. A. (1979) *Biochem. Biophys. Res. Commun.* **88,** 274–280
7. Schaefer, J. & McKay, R. A. (1999) U.S. Patent 5861748
8. Griffin, R. G. (1998) *Nat. Struct. Biol.* **5,** 508–512
9. Gullion, T., Baker, D. B. & Conradi, M. S. (1990) *J. Magn. Reson.* **89,** 479–484
10. Morris, G. A. & Freeman, R. (1978) *J. Magn. Reson.* **29,** 433–462
11. Bork, V. & Schaefer, J. (1988) *J. Magn. Reson.* **78,** 348–354
12. Saitô, H. (1986) *Magn. Reson. Chem.* **24,** 835–852
13. McDowell, L. M., Schmidt, A., Cohen, E. R., Studelska, D. R. & Schaefer, J. (1996) *J. Mol. Biol.* **256,** 160–171
14. McDowell, L. M., Poliks, B., Studelska, D. R., O'Connor, R. D., Beusen, D. D. & Schaefer, J. (2004) *J. Biomol. NMR* **28,** 11–29
15. Skokut, T. A., Manchester, J. & Schaefer, J. (1985) *Plant Physiol.* **79,** 579–583
16. Skokut, T. A., Varner, J. E., Schaefer, J., Stejskal, E. O. & McKay, R. A. (1982) *Plant Physiol.* **69,** 308–313
17. Mesnard, F. & Ratcliffe, R. G. (2005) *Photosyn. Res.* **83,** 163–180
18. Douce, R., Bourguignon, J., Neuburger, M. & Rébeillé, F. (2001) *Trends Plant Sci.* **4,** 167–176
19. Noctor, G. & Foyer, C. H. (1998) *J. Exp. Bot.* **49,** 1895–1908
20. Bunce, J. A. (1998) *Plant Cell Environ.* **21,** 115–120

21. Wishart, D. S. & Sykes, B. D. (1994) *Methods Enzymol.* **239,** 363–392
22. Laws, D. D., Bitter, L. H.-M., Liu, K., Ball, H. L., Kaneko, K., Wille, H., Cohen, F. E., Prusiner, S. B., Pines, A. & Wemmer, D. E. (2001) *Proc. Natl. Acad. Sci. U. S. A.* **98,** 11686–11690
23. Cassab, G. I. (1998) *Annu. Rev. Plant Physiol. Mol. Biol.* **49,** 281–309
24. Prentice, I. C. (2001) in *Climate Change 2001: The Scientific Basis* (Houghton, J. T., Ding, Y., Griggs, D. J., Noguer, M., van der Linden, P. J., Dai, X., Maskell, K. & Johnson, C. A., eds), pp. 183–238, Cambridge University Press, Cambridge, UK
25. Drake, B. G., Gonzalez-Meier, M. A. & Long, S. P. (1997) *Annu. Rev. Plant Physiol. Plant Mol. Biology* **48,** 609–639
26. Farage, P. K., McKee, I. F. & Long, S. P. (1998) *Plant Physiol.* **118,** 573–580
27. Rogers, A., Allen, D. J., Davey, P. A., Morgan, P. B., Ainsworth, E. A., Bernacchi, C. J., Cornic, G., Dermody, O., Dohleman, F. G., Heaton, E. A., Mahoney, J., Zhu, X.-G., Delucia, E. H., Ort, D. R. & Long, S. P. (2004) *Plant Cell Environ.* **27,** 449–458
28. Rachmilevitch, S., Cousins, A. B. & Bloom, A. J. (2004) *Proc. Natl. Acad. Sci. U. S. A.* **101,** 11506–11510

Glycine Metabolism in Intact Leaves by *in Vivo* 13C and ^{15}N Labeling

Lynette Cegelski and Jacob Schaefer

J. Biol. Chem. 2005, 280:39238-39245.
doi: 10.1074/jbc.M507053200 originally published online September 13, 2005